Interlaminar Tensile Properties of Unidirectional and Woven Carbon Fiber Reinforced Toughened Epoxy Laminates

A Senior Project
Presented to
the Faculty of the Materials Engineering Department
California Polytechnic State University – San Luis Obispo

In Partial Fulfillment
of the Requirements for the Degree
Bachelor of Science in Materials Engineering

By

Eric Casey and Sean Thompson
Advisor: Dr. Blair London
Sponsor: Toray Advanced Composites

June 2023

Acknowledgements

We would like to thank Dr. Blair London, Cal Poly Materials Engineering Department for serving as our project advisor throughout this project.

We would like to thank Eric Beaton for his troubleshooting and maintenance work on the equipment we have available in the Materials Engineering Department.

We would like to thank Toray Advanced Composites for sponsoring this project and specifically Mason Souther, William Shiu, and Wyatt Taylor for their guidance and providing excellent resources to the project.

Abstract

This project aims to develop a dataset on interlaminar tensile strength comparing unidirectional and woven thermoset matrix carbon fiber composites keeping ply count, matrix material, and fiber diameter constant. The interlaminar tensile strength is an important property relating to the delamination failure mode. Interlaminar tensile strength is determined using the ASTM D6415 testing standard. This test is a modified four-point bend test using a 90° curved beam test specimen. Laminates were produced by laying up pre-impregnated carbon fiber sheets onto a curved beam tooling. The unidirectional laminate was produced with 20 plies in a $[0,0,90,0,0]_4$ layup pattern. The woven fiber laminate was produced with 20 plies of a 2x2 twill weave fabric in the 0° orientation. Both laminates were cured in an autoclave. The laminate panels were machined into the test specimens with a width of 1 inch. The ASTM D6415 tests were performed with a crosshead displacement rate of 2.0 mm/min until there was a drop in load indicating initial delamination. The unidirectional specimens had an average interlaminar tensile strength of 8.72 Ksi. The woven fabric specimens had an average interlaminar tensile strength of 9.52 Ksi. After testing, the specimens were sectioned and imaged using optical microscopy and scanning electron microscopy (SEM). The specimens for SEM were gold sputter coated and imaged under high vacuum mode. Imaging indicated that for unidirectional specimens, delamination started in the matrix then propagated along the ply boundary. Woven specimens appeared to fail in regions of excess matrix material at intersections of fiber orientations. It is recommended for continuing work to use a test fixture that does not need to be offset. It would also be beneficial to have adjustable span lengths for the top and bottom jaws to increase specimen compatibility. Lastly, increasing matrix toughness would increase failure loads where stress concentrations are common in components.

Key words: Materials Engineering, carbon fiber reinforced polymer, pre-impregnated, thermoset matrix, unidirectional laminate, woven laminate, delamination, interlaminar tensile strength, autoclave, scanning electron microscopy.

Table of Contents

List of Figures

List of Tables

1. Introduction

Toray Advanced Composites, in Morgan Hill, California; designs, manufactures, and supplies fiber reinforced polymer composites for a broad spectrum of industries and applications. Toray has been developing high-performance thermoset matrix carbon fiber composites. The interfacial quality of these high-performance composites needs to be validated so that Toray can uphold their reputation as one of the leading composites suppliers in the country. The aim of the project is to introduce the ASTM-D6415 test standard as a quality assurance test for the interlaminar tensile strength (ILTS) of carbon fiber reinforced polymer (CFRP) laminates. Woven and unidirectional CFRPs will be compared to experimentally examine their benefits and drawbacks with respect to interlaminar tensile properties. Prior work has shown that delamination through shear or tensile mechanisms is a common failure mode for laminated CFRP components, leading to the importance of this project. This project will use the ASTM-D6415 standard test to determine the failure modes and ILTS of the woven and unidirectional laminates. There are many variables that affect the ILTS results which makes controlling the loading and manufacturing quality of specimens necessary.

1.1 Industry Overview

The CFRP industry has steadily grown due to the high strength to weight ratio that the material provides. These properties have led to in use in aerospace, wind energy, automotive, and pressure vessels. The recreational use of carbon fiber composites has also been increasing with high performance sporting equipment using the material. Carbon fiber demand is expected to grow 10% annually[1].

1.2 Carbon Fiber Reinforced Polymer Overview

1.2.1 Producing CFRPs

CFRP's are produced from carbon fibers and held together with a polymer matrix. The carbon fibers are impregnated with a polymer. Fiber impregnation can be done during component production or by the manufacturer. Manufacturers introduce resin in the fibers to form sheets of pre-impregnated fiber (prepreg). The resin is added to the fibers in a controlled and uniform manner resulting in a uniform matrix content in the final material[2,3].The prepreg sheets will then be cut and stacked before being cured. The components are typically cured in an autoclave at elevated temperature and pressure (Figure 1). This process results in consistent high-quality components; it is also efficient for large scale production. The major drawback to prepreg material is the added costs during production. The polymer matrix in prepreg is in a semi-cured state that must be refrigerated until it is used[3]. Prepreg is also less workable than loose fibers and makes complex geometries more difficult to produce than other production methods[3].

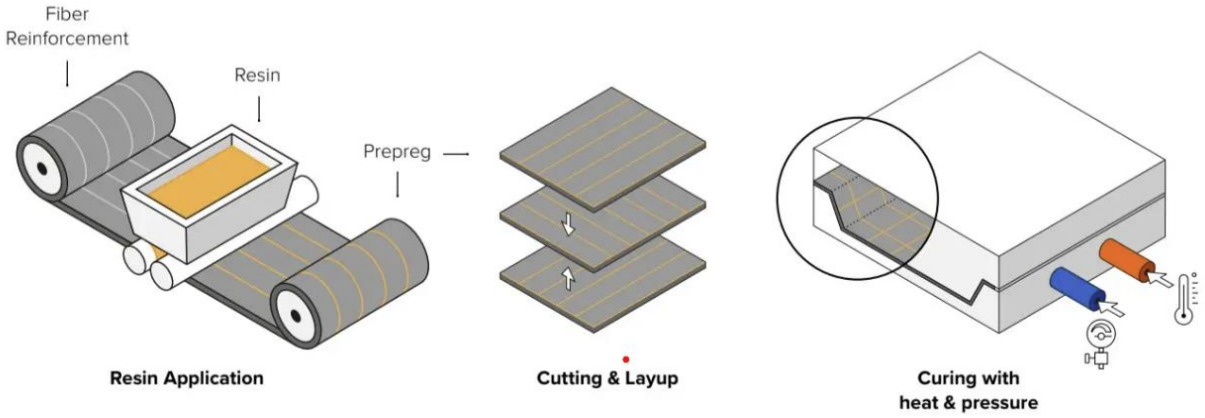

Figure 1: Production process of prepreg plies and CFRP components[3].

1.2.2 Matrices in Fiber Reinforced Composites

The matrix in CFRP materials has significant implications on the applications of the material. The primary function of the matrix material is to distribute loads between the fibers [4]. The matrix also will determine the chemical resistance and the operating temperature for the composite materials [5]. There are two main classes of polymer matrices: thermosets and thermoplastics. Thermoset polymers are currently the most used class of polymers for CFRPs. This is due to the low viscosity resins, high service temperatures, and superior mechanical properties. The low viscosity of thermoset resins allows for room temperature processing with little need for specialized equipment [6,7]. The high service temperature enables more applications for the materials [4–6]. Finally, thermosets have higher modulus, strength, and creep resistance than thermoplastics because of their crosslinked structure[5]. The most common thermoset matrix materials are epoxies, polyesters (unsaturated and vinyl), and phenolic resins [8]. The epoxy resins are used for high performance applications such as aircraft components. This is due to the low shrinkage during curing and the ability to modify the properties with changes to the formulation (Figure 2) [7,9]. Polyester is the most used matrix in CFRPs due to a balance of cost, material properties, and workability [5]. Carbon filled phenolic resins can be used for rocket nozzles due to their flammability properties, low heat transfer, and high chemical and thermal resistance[9] (Figure 2b).

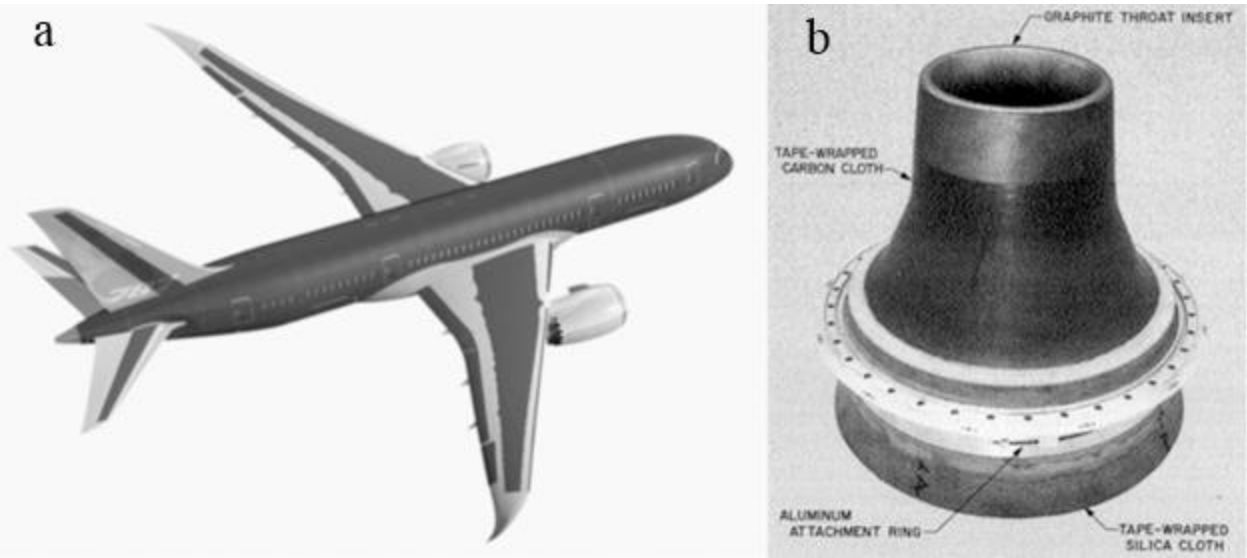

Figure 2: (a) The Boeing 787 uses 50% CFRP using an epoxy matrix for most of the composite material[10]. (b) A rocket nozzle that uses a phenolic resin matrix reinforced by a carbon fiber cloth[11].

1.2.3 Role of Carbon Fibers in Fiber Reinforced Polymers

The carbon fibers used in CFRPs are bonded together by the matrix material and provide the strength and stiffness of the composite. Carbon fibers can be produced from three main precursors: polyacrylonitrile (PAN), rayon, and pitch. The final properties of the fibers are dependent on the orientation of the crystal structure. PAN is the most common precursor for carbon fiber and can produce the best material properties[12].

The production of all carbon fibers follows a similar process. The precursor first undergoes fiberization, where the material is drawn into fiber tows. Fiber tows are strands of numerous fibers with fiber counts ranging from 1,000 to 24,000 individual fibers per tow. This is typically done through dry, wet or melt spinning; before being drawn into the fiber. Next, a stabilization step is performed to prevent the precursor from melting in subsequent treatments. Stabilization involves heating the fibers under atmospheric conditions to produce a protective oxide layer on the fibers. The next step, carbonization, heats the fibers to 1000-1500 ℃ under an inert atmosphere. This increases the carbon content of the fibers to >90%. A final step, graphitization, may be performed to further increase the carbon content and alignment of the crystal structures. This is done by heating the fibers to an even higher temperature. The temperature of the final heat treatment is adjusted to achieve the desired mechanical properties[12] (Figure 3). PAN fiber precursors are made into carbon fibers with a multistage heating and drawing process (Figure 4).

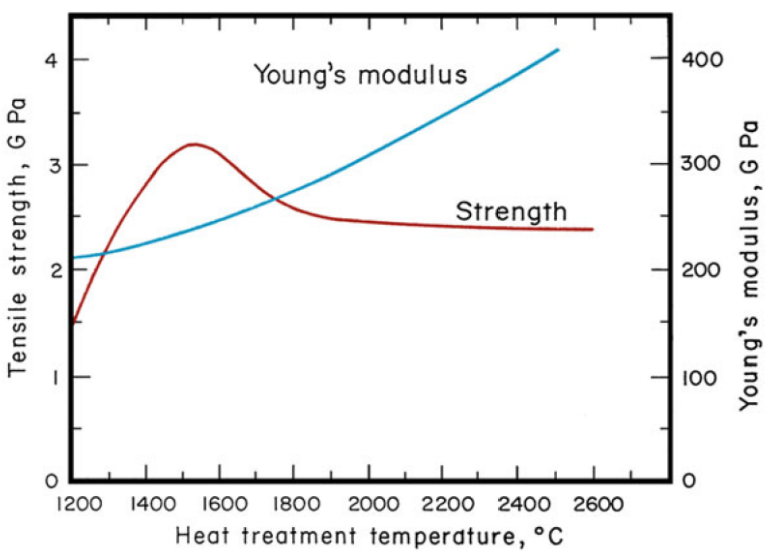

Figure 3: Strength and elastic modulus as a function of final heat treatment for PAN based carbon fibers[13].

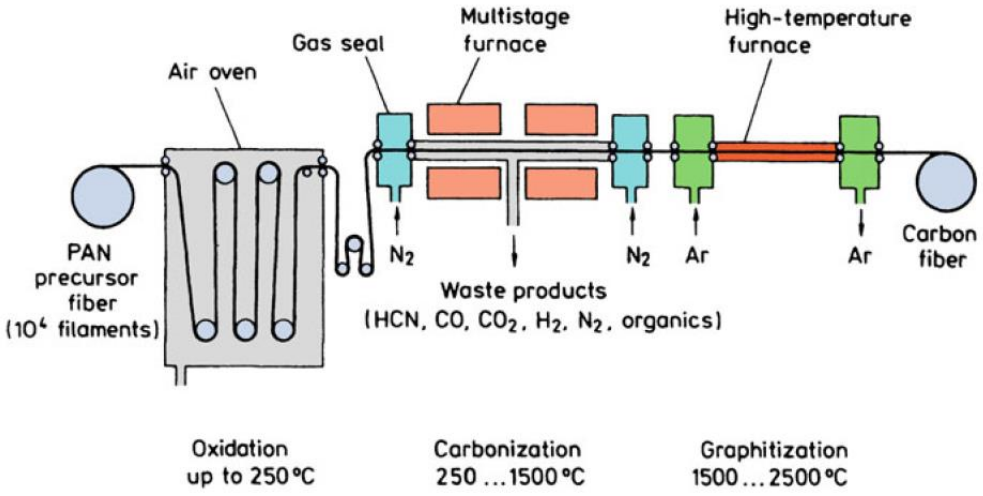

Figure 4: Schematic of carbon fiber production from the PAN precursor[12].

1.2.4 Effects of Fiber Orientation

Carbon fibers are anisotropic materials with the highest strength and stiffness in the direction of the fibers. To achieve optimal performance the design of components must account for the orientation of the carbon fiber. In applications that require strength in more than one direction, fibers with varying orientations can be used to produce a final laminate that has excellent mechanical properties in multiple directions. The need for different fiber orientations complicates the manufacturing of the components. The stiffness of the fibers will also make complex geometries more difficult to produce. When designing carbon fiber components, layers of unidirectional fibers can be used. Unidirectional fibers will have ideal mechanical properties as the fibers can be placed in optimal orientations for the component. However, unidirectional fibers do not conform to complex geometries easily[14].

Another option is to use layers of carbon fiber fabrics. Most fabrics are woven with interlacing perpendicular tows of fiber. The tows of fiber that run lengthwise are called the warp tows while the tows that run perpendicular are called the weft tows. There are many common weave patterns that will perform better for various geometries. Plain weave fabrics have a checkerboard pattern, with the tows woven in an over/under pattern. This results in a stable laminate with well-maintained fiber orientations. Plain weave fabrics are most suitable for flat panels as the stability prevents the fabric from contouring. Another common weave is the twill weave (Figure 5). The most common twill weave is the 2x2 twill weave. The 2x2 twill weave pattern has a two-by-two weave where two warp tows pass over two weft tows. The tows interlacing in a twill weave produce the diagonal rib pattern and is the most popular weave for decorative purposes[15]. The twill weave also has far superior drapability when compared to a plain weave or unidirectional fibers and is often used for components with compound curves.

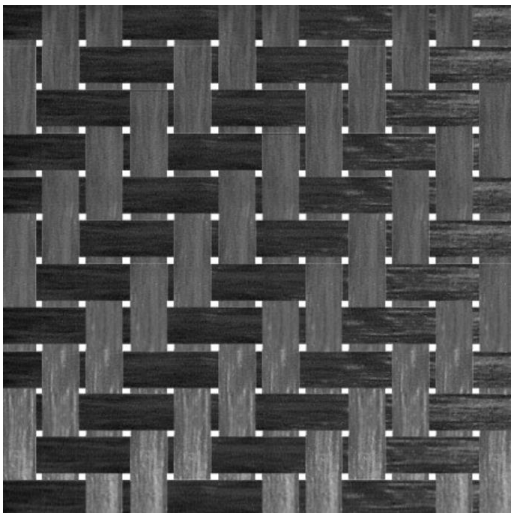

Figure 5: 2x2 Twill weave pattern resulting in the diagonal rib pattern[15].

1.2.5 Interface of Carbon Fibers and Polymer Matrix

The interphase/interface is defined as a region where the fiber properties differ from the properties of the bulk fiber, and the matrix properties differ from the properties of the bulk matrix, representing a region of mixed properties between fiber, matrix, fiber-matrix adhesion and other constituents. As the matrix distributes load between fibers in a carbon fiber composite laminate, each fiber and its surrounding matrix must have a good interface to effectively transfer load from matrix to fibers. The interface is typically a mechanically weaker phase than the matrix or fiber itself. Compositionally, in thermoset epoxy matrix carbon fiber composites, the interphase is made up of, sizing crosslinking agents, cured epoxy resin, physiosorbed materials – typically carbon dioxide and/or water, coupling agents, finishers, and primers [16–18]. Transmission Electron Microscopy (TEM) can be used to characterize the interface region in size and the gradient of constituent phases are shown to be more carbon-rich nearest the fibers (Figure 6).

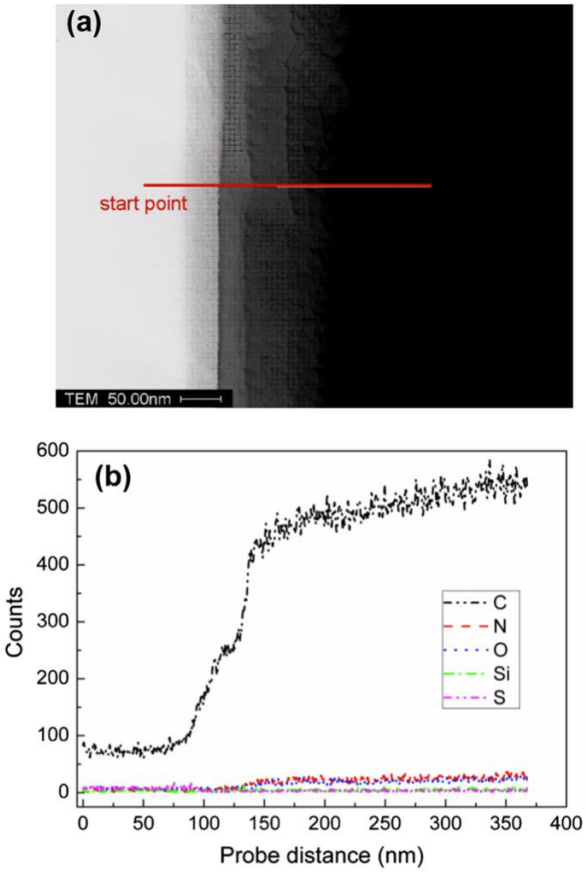

Figure 6: (a) TEM image of carbon fiber/epoxy with red line denoting the linear scan (b) Atomic counts of elements as a function of probe distance.[19]

This composite of materials in the interface region impacts the material properties of the overall carbon fiber composite. The effect of the interface's micromechanics on the overall composite can be achieved by regulating the composition, structure, and distribution of the matrix-fiber interphase of carbon fiber composites. Improving the chemical bonding between matrix and fibers through sizing is important to increase matrix/fiber compatibility and interfacial quality (Figure 7). Besides serving as a protective coating for the raw fibers, sizing contains critical adhesive agents that improve the load transfer properties between fibers and matrix. [20]

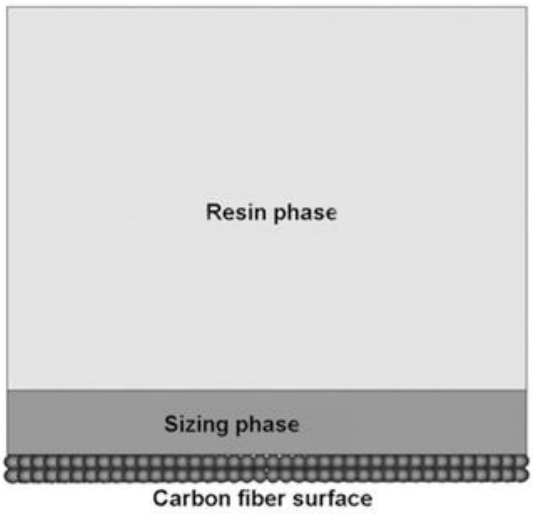

Figure 7: Diagram of interphase constituents in carbon fiber composites.[19]

This interfacial region is currently being heavily researched in literature and is a growing area with potential for large improvements in the properties of laminates, namely adhesion and delamination in carbon fiber composites.

1.2.5.1 Mechanical properties of the Interface

A substantial subset of mechanical properties of carbon fiber reinforced polymers depends on the interfacial adhesion quality between fiber and matrix material. Specifically, the interphase region is shown to have a large effect on the impact toughness and off-axis strength. However, bulk properties such as failure stress and shear strength are also significantly impacted by the interphase region, due to the coupling agents in the sizing that increase bonding strength to the matrix and the carbon fibers. Sizing also produces a roughening effect on the fibers that increases the surface area to bond the carbon fibers with the matrix. Sizing also helps to achieve good wetting of the resin throughout the fibers, facilitating the impregnation process and achieving efficient load transfer among the fiber tows. Interlaminar properties of composite laminates are also greatly impacted by the interphase region. The interlaminar tensile strength can be much lower in the interphase region than in the fiber direction, so small areas of poor interfacial quality can have a notable impact on the overall mechanical properties of the laminate. Advancements in the understanding of carbon fiber composite interphases have revealed that composite properties are controlled by fiber, matrix, and interphase properties.

1.2.5.2 Surface Treatments and Effects

Surface treatment methods are commonly used in carbon fiber applications to improve the interfacial properties of the carbon fiber laminate. The graphitic basal planes of carbon fiber are mostly non-polar and chemically inert so they will not form strong bonds with polar matrices such as epoxy resin. Surface treatments serve to increase the amount of active carbon on the surface to react with matrix material. They also increase the surface roughness and wettability of the fibers. The interphase region’s mechanical properties can be improved by electrolysis (anodic oxidation of the surface) and sizing. Sizing is a thin coating applied to fibers during

manufacturing that protects them during processing and handling. The improvement in the material properties is due to sizing and electrolysis' coupled effect on increasing the maximum wettability and chemical bonding between fiber and matrix [18]. Surface oxidation treatments of carbon fibers, while increasing chemical bonding between fiber and matrix have the pitfall of potentially over-oxidizing and oxidatively embrittling the fibers themselves. Another factor that improves adhesion strength is surface roughening which increases physical bond strength to the matrix, by increasing surface area for the matrix to bond to the fibers, and the overall physicochemical compatibility. Conversely, it has been shown that over 200℃ temperature heat treatment of the fibers can weaken the mechanical properties of the interphase. This was attributed to a significant decrease in chemical bonding between the fiber and matrix but an increase in surface roughness [18]. The type and concentration of sizing agent also was shown to play a role in the surface roughness improvement. Sizing agents are meant to increase the chemical bonding between fiber and matrix, but evidence has shown that they have some impact on surface roughness and wettability of the fibers, which also improves adhesion[18,21].

1.2.5.3 Characterization of Surface Treatments

Due to the complex nature of adhesion between the fiber and the matrix, interfacial properties are complicated to characterize. Categorizing, predicting, and controlling the quality of the interphase allows for great improvements in carbon fiber composites. The interphase region is examined in the literature using many different characterization techniques. Atomic Force Microscopy (AFM) or Scanning Electron Microscopy (SEM) is used to detect changes in and existing morphology, Fourier Transform Infrared Spectroscopy (FTIR) is useful to find relative amounts of each atomic constituent approaching the fiber from the matrix, Young's contact angle testing with glycol and water to quantify hydrophilicity/hydrophobicity, nuclear magnetic resonance imaging to obtain microscopic images of liquids, and flexible molecules. FTIR can also be used to characterize the concentration of sizing, bonding patterns, chemical behavior, degradation, and more (Figure 8).

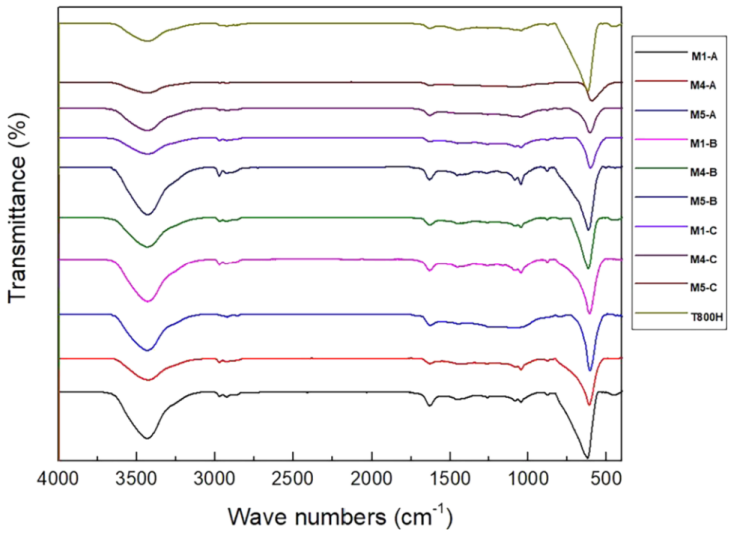

Figure 8: FTIR spectra of various CF with differing sizing content.[21]

When fabricating carbon fiber composites, the fibers interphase region has been found to extend anywhere from 1-1000 nm radially from the edge of the bulk fiber. Therefore, with thousands of filaments in the tows that make up carbon fiber layers in a composite ply, a sizable portion of the overall composite is interphase region and thus controlled by interphase properties and mechanics [16]. Bulk characterization effectively has left interfacial properties to be ignored due to the dilution of their effect in the bulk[16]. Interfacial properties become crucial in preventing delamination related failures, and improving these properties improves overall adherence between layers and more effective load distribution.

1.3 Mechanical Testing of Carbon Fibers

Carbon fiber's mechanical properties are determined through several common testing methods. Among these methods include short beam shear, bend, and tensile – both in-plane and transverse to fiber orientation.

1.3.1 Bend Testing

Bend testing of composites is important to find the flexural stiffness and strength of a carbon fiber composite. Bend tests apply bending moments which can be seen as tensile and shear forces that act on the test specimen (Figure 9a). Important test results include deflection angle or distance which determines the test specimen elasticity, and fracture strength in bending is critical for composite parts that will undergo a bending moment in application. Short beam shear is heavily used in industry to determine shear strength and thus quality of a particular layup of carbon fiber because of its ease of setup and ease of producing test specimens (Figure 9b).

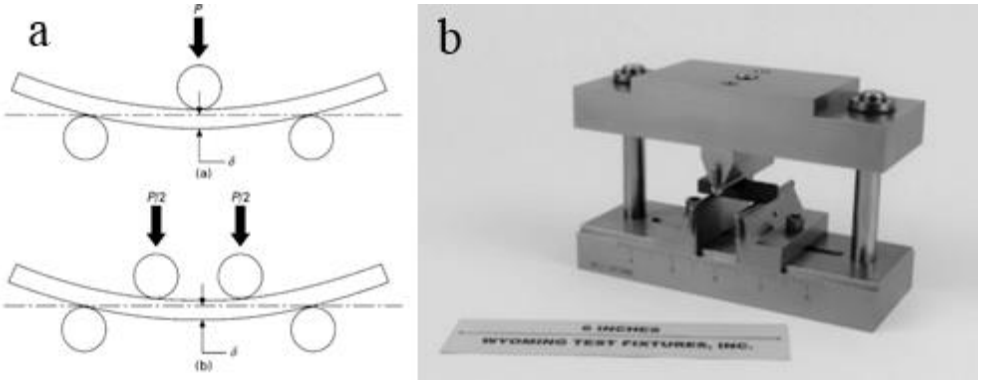

Figure 9: (a) 3 and 4-pt bend test diagrams and (b) Wyoming Test Fixture's short beam shear test fixture.

This short beam shear test method is used as a quality verification measure across specimens from the same layup to identify process defects that cause variation in shear strength results. The short beam shear test applies a 3-point bending load across a small span length to maximize shear and minimize tension forces applied by the bending test apparatus. The commonly used CRAG100 test standard calls for a length of 20 mm span length of 5x thickness and a thickness that is as close as possible to 2 mm for materials with a flexural strength to shear strength ratio of at least 10:1.[22]

1.3.2 Interlaminar Tensile Testing

ILTS is an important material property for composite laminates as a common early source of failure and thus a quality assurance issue for the composites industry can be found in the interphase region between laminates. ILTS is defined as the tensile strength through the thickness, or between plies of a composite laminate. ILTS can be found in a few separate ways and are referenced in the literature by two different methods – indirect and direct loading. Direct loading involves an out of plane tensile load applied to the top and bottom of a sandwich panel. In the literature, there are two ASTM standards on test methods for this. ASTM D7291 deals with cylindrical and circular test specimens, while ASTM C297 deals with rectangular test specimens [23,24]. Alternatively, the latter mentioned indirect loading methods involve imposing a bending moment on a curved beam test specimen (Figure 10a) (Figure 10b). The test method most critical to our project's experimentation determines ILTS indirectly using a 4-point bend test to apply an indirect load, which then causes a bending moment that induces a tensile force as well as some amount of shear. This method is further expanded on in the ASTM D6415 standard for mechanical testing of composites [25]. A substantial concern for this test method is that the ILTS test is ended in most cases by specimen failure, and the test specimen's quality highly impacts failure mode and failure strength, and thus the ILTS is not fully determinable by ASTM D6415 testing alone. This test is most useful in industry as a supplemental quality verification test to collect data on the quality of the adhesion of fiber layers and matrices in batches across the same manufacturing process (Figure 10c).

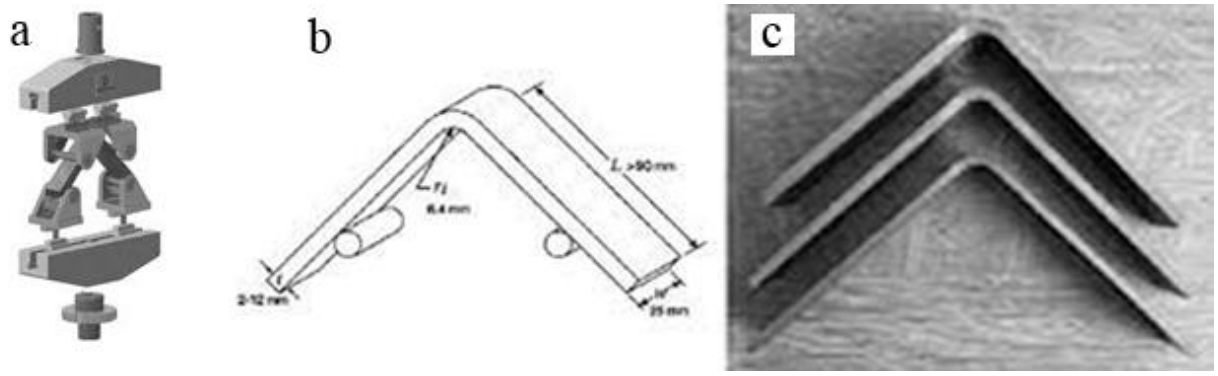

Figure 10: ASTM D6415 (a) test fixture diagram[26] and (b) test specimen diagram[27] and (c) test specimen of varying widths.[27]

2. Project Overview

Toray Advanced Composites is sponsoring an investigation into comparing a unidirectional and woven toughened epoxy matrix reinforced by T1100G and T800SC carbon fibers respectively. These fibers have the same fiber diameter, so they are comparable in interfacial areas with the toughened epoxy matrix which is a primary contributor to the ILTS results. The matrix material being used for both laminates is the TC380 toughened epoxy. The ply adhesion quality, toughness of the matrix, and ILTS will be examined for each laminate construction through the ASTM-D6415 test and analysis of the failure modes that occur. The ASTM D6415 test gives data that represents the performance of the material in components with complex geometries more closely than other testing methods. This project aims to help improve the design process for components with complex geometries and stress states.

3. Methodology

3.1 Test Specimen Preparation

The ASTM D6415 test requires a curved beam test specimen. The 20-ply unidirectional specimens were produced using a [0°,0°,90°,0°,0°] fiber orientation scheme with 4 repetitions of this pattern to produce a 20-ply laminate. The plies were 8″ long by 12″ wide. Individual plies were stacked until one repetition of the pattern was completed (Figure 11). Afterwards, a 15-minute debulk was performed to aid in consolidation (Figure 12). Once all plies were laid up onto the curved beam tooling, a final 15 minutes debulk was performed, and the panel was ready for an autoclave cure. After the autoclave cure was complete, the laminate was sectioned into individual test specimen with a width of 1″ (Figure 13)

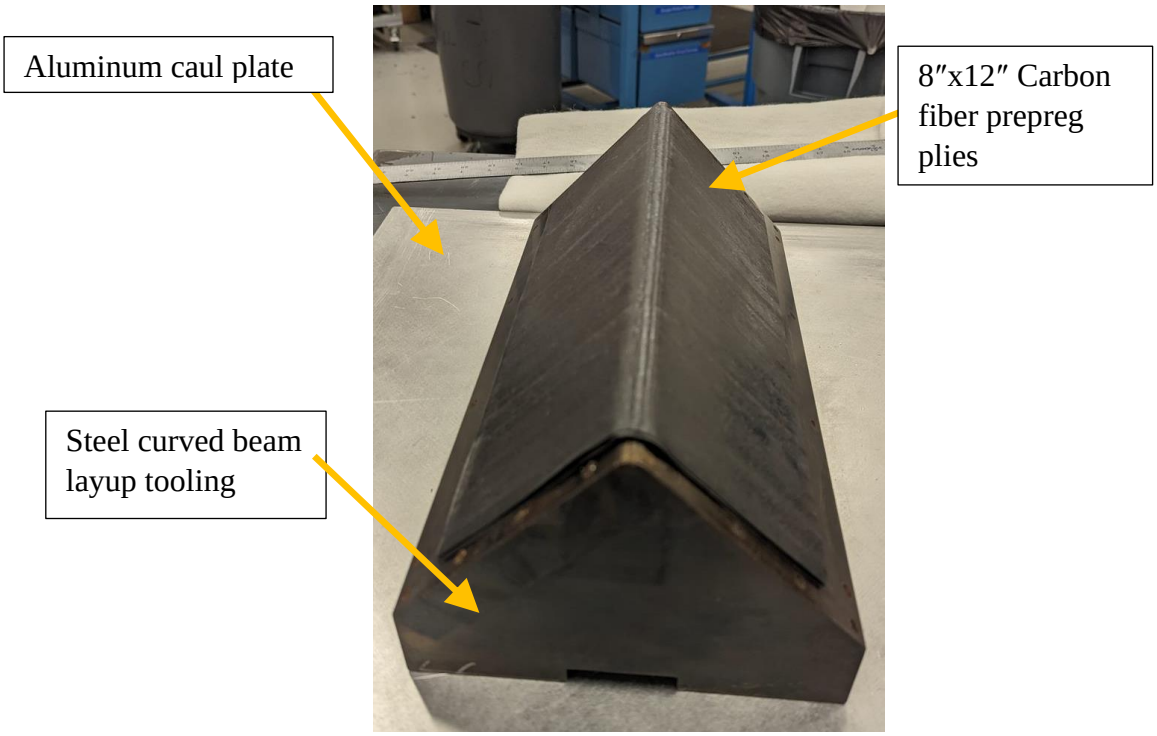

Figure 11: Unidirectional layup during ply stacking.

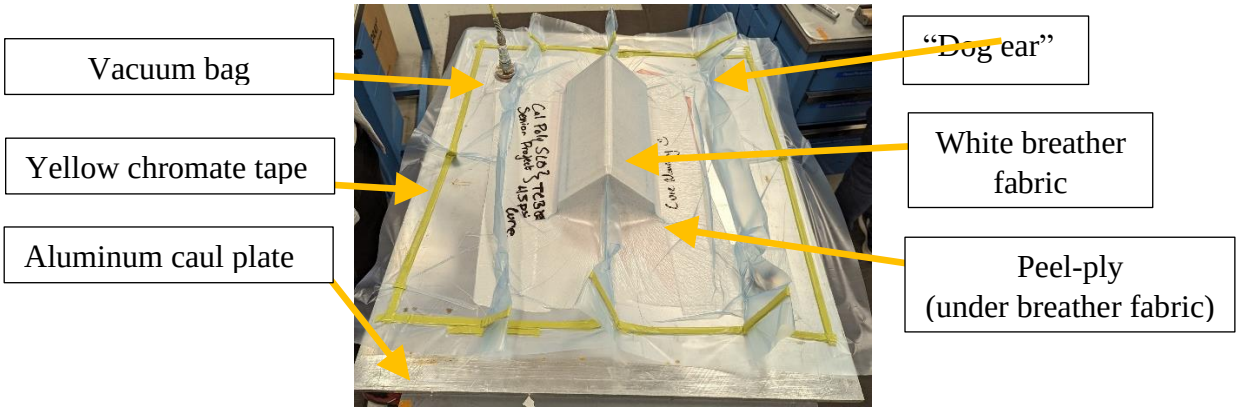

Figure 12: Unidirectional layup under vacuum during the final debulk. The peel-ply is laid over the prepreg, followed by the breather fabric. The vacuum bag is then laid over the entire caul plate and sealed to the plate using chromate tape. "Dog ears" are folds of excess bagging material incorporated to reduce stress on the vacuum bag while a vacuum is pulled.

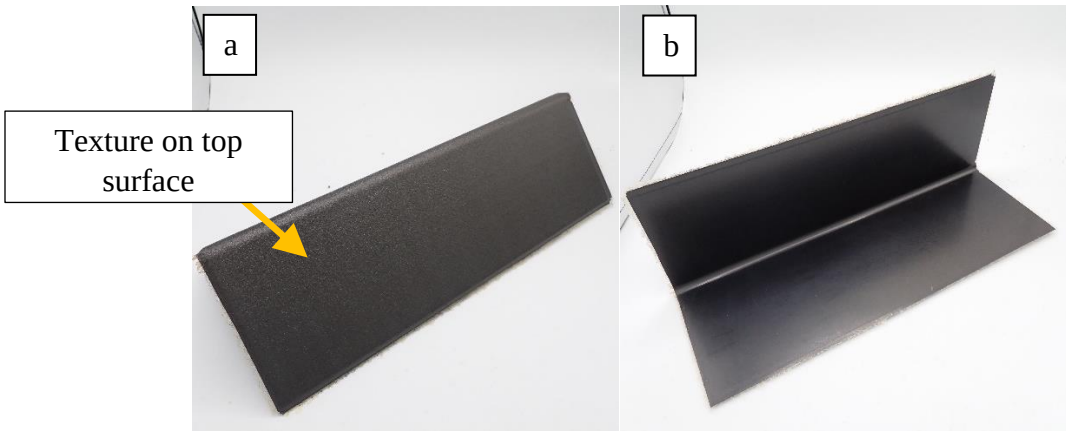

Figure 13: Cured unidirectional laminate before being machined into test specimens. Showing the top surface (a) and bottom surface (b). The texture of the top surface is from the breather fabric used to absorb excess resin.

The woven fabric specimens were laid up similarly with 20 plies of a 2x2 twill weave prepreg with intermittent debulks. The woven panel was laid up all in a [0°] orientation to produce the 20-ply laminate. The laminate was also cured using an autoclave and machined to 1" wide test specimen.

3.2 ASTM D6415 Testing

This project used the ASTM D6415 testing standard to induce delamination in the test specimen and determine the ILTS for the composite laminates. To perform the ASTM D6415 testing, a test method was set up within the Bluehill software using a 2 mm/min displacement rate. The test end condition was set as a drop to 50% of maximum load. A sudden drop in load indicates a delamination has occurred. The testing was performed using a 150 kN Instron load frame. The ASTM D6415 test fixture provided by Toray Advanced Composites needed an adaptor to produce a horizontal offset that provided sufficient clearance for the top and bottom jaws.

(Figure 14). The specimen was placed in the jaws and carefully centered with the upper jaw to prevent side-loading and ensure proper application of forces during test. Eight specimens of unidirectional and woven carbon fiber laminates were tested to determine an average ILTS.

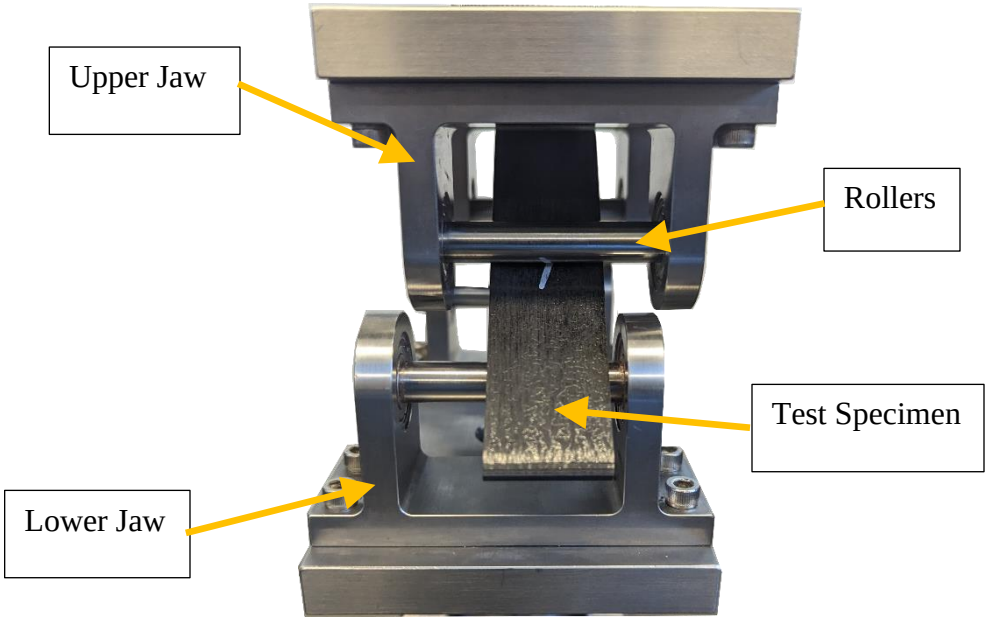

Figure 14: The offset needed to allow clearance for the ASTM D6415 test fixture, shown with a test specimen centered with the upper fixture jaw.

3.3 Optical Microscopy

To view the specimens optically, we first machined the specimen so that the bend region could be analyzed. The bend regions were mounted in clear acrylic, ground and polished to 0.5 μm by using MicroCloth with alumina suspension as the polishing media. After polishing, the mounted specimens were rinsed and dried to be imaged.

3.4 Scanning Electron Microscopy

To be prepared for SEM, the test specimens were sectioned using a Dremel to approximately 1 cm^2. The specimens split apart along a delamination during this process and thus were able to be imaged in a top-down view to see both halves of the fracture surface. The specimens were then mounted on the SEM specimen holders and sputtered with gold. Sputtering was essential to image the non-conductive specimen under high vacuum mode. Two unidirectional and one woven specimen were prepared in total for SEM imaging.

4. Results

4.1 Unidirectional Fiber ASTM D6415 Testing

The test data was recorded using the Bluehill software on the 150 kN Instron load frame. The ASTM D6415 tests resulted in delamination occurring at 400-500 pounds with a crosshead displacement of 0.35-0.45″ for the unidirectional specimens (Figure 15).

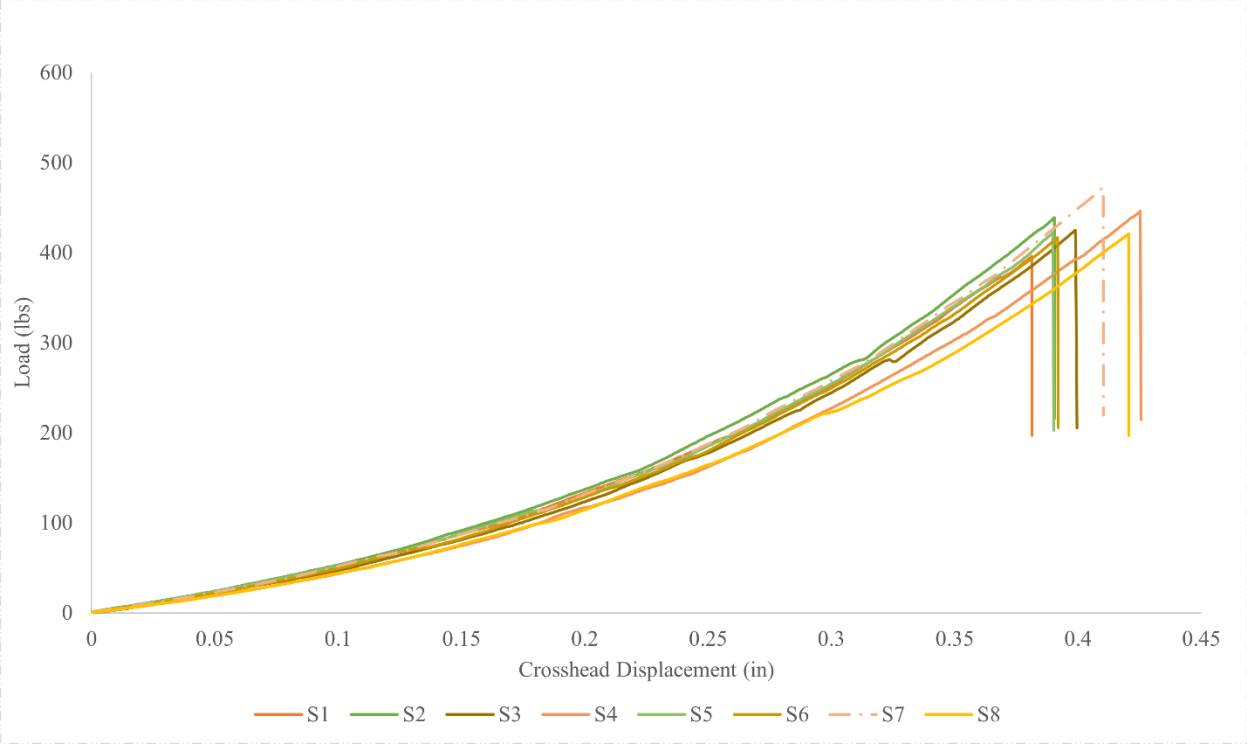

Figure 15: Unidirectional fiber ASTM D6415 test data showing initial delamination occurring between 0.35-0.45″ at loads of 400-500 lbs. Specimen 7 (dashed line) was tested using a 50 kN Instron.

During testing, the 150 kN Instron load frame went down, and specimen 7 had to be tested using a smaller 50 kN Instron. While testing with the smaller load frame an issue became apparent with the test setup. The smaller load frame would shift during testing due to a front to back misalignment caused by the adapters needed to produce the offset. Specimen 7 reached the highest load before delamination.

4.2 Woven Fiber ASTM D6415 Testing

The woven fiber ASTM D6415 testing produced a spread in load required to cause delamination ranging from 600-800 lbs. The delamination occurred between 0.3 and 0.35″ (Figure 16). To test the woven fiber specimen the 50 kN Instron was initially used. The fixture shifting resulted in the specimen slipping off the fixture before delamination. Only one specimen delaminated while using the 50 kN Instron. Once the 150 kN load frame was operational again, the remainder of the specimens were able to be tested. The misalignment that was first noticed on the 50 kN load frame was still present, but the stiffer frame was able to withstand the off axis loading and delaminate the specimen. The specimen had also experienced substantial loading from the 50 kN testing which could affect the results.

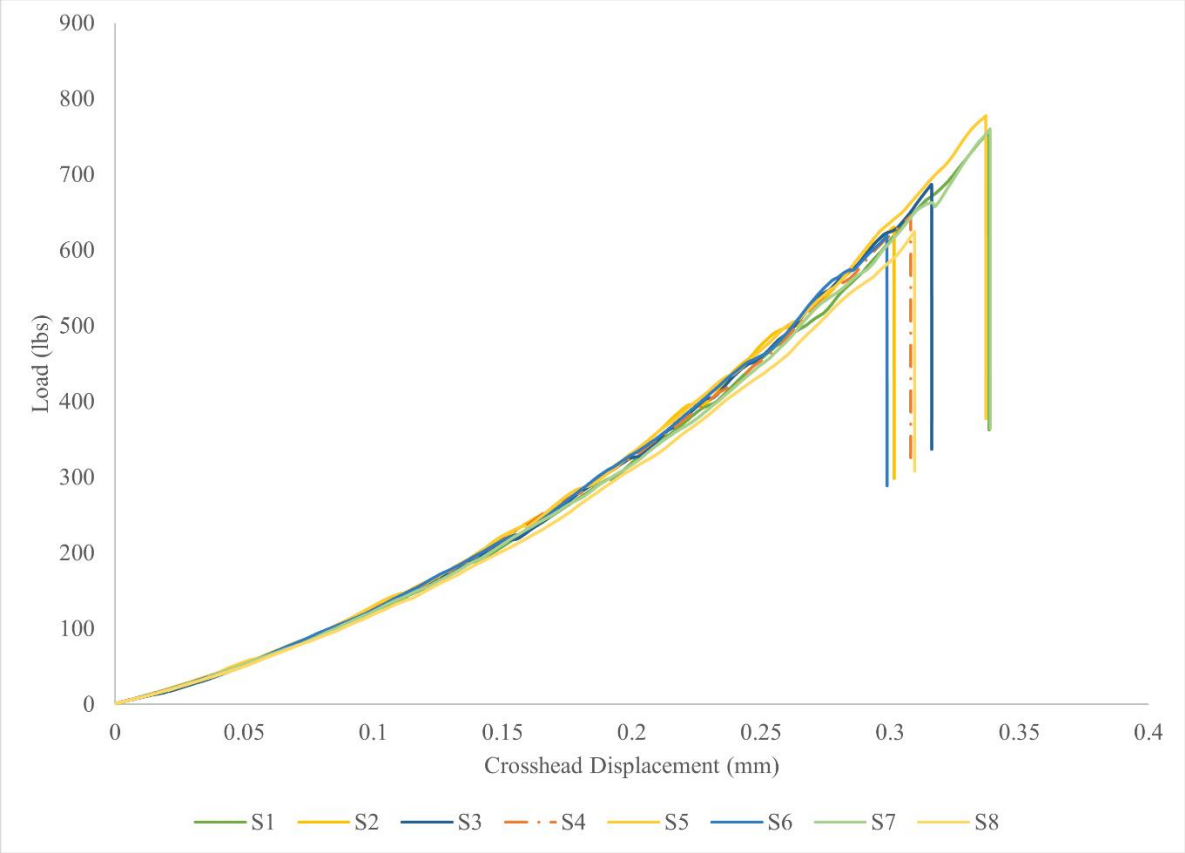

Figure 16: ASTM D6415 testing for the woven fiber specimen. Delamination occurred at loads between 600-800 lbs and a crosshead displacement of 0.3-0.35″. Specimen 4 (dashed line) was performed on the 50 kN load frame. All tests showed more variance in loading force than the unidirectional specimen.

4.3 Interlaminar Tensile Strength Data

The maximum load values that corresponded to the initial delamination were used to calculate curved beam strength, which is defined as the moment per unit width which causes a delamination to form[25]. The curved beam strength is given in (1) where φ is the angle in degrees of the loading arm from horizontal, d_x is the horizontal distance between the centerlines of two top and bottom adjacent rollers. D is the diameter of the cylindrical loading bars, and t is the specimen thickness.

$$CBS = \frac{P}{2w * \cos(\varphi)}\left(\frac{d_x}{\cos(\varphi)} + (D + t) \cdot \tan(\varphi)\right) \quad (1)$$

The interlaminar tensile strength values were calculated from the curved beam strength using (2). σ_r^{max} is the maximum radial stress which is equivalent to the ILTS with an error of less than 2 % [25], r_i is the inner radii of the curved segment, and r_o is the outer radii of the curved segment.

$$\sigma_r^{max} = \frac{3 \cdot CBS}{2t\sqrt{r_i r_o}} \quad (2)$$

The interlaminar tensile strength was calculated for the unidirectional and woven fiber specimen (Figure 17). The unidirectional specimen showed more consistent values with ILTS values between 8.25 and 9.5 Ksi. The ILTS values for the woven fiber specimen ranged from 8.5-10.25 Ksi. The average maximum load, crosshead displacement, curved beam strength, and interlaminar tensile strength for the unidirectional fiber and woven fiber specimen are displayed in Table I.

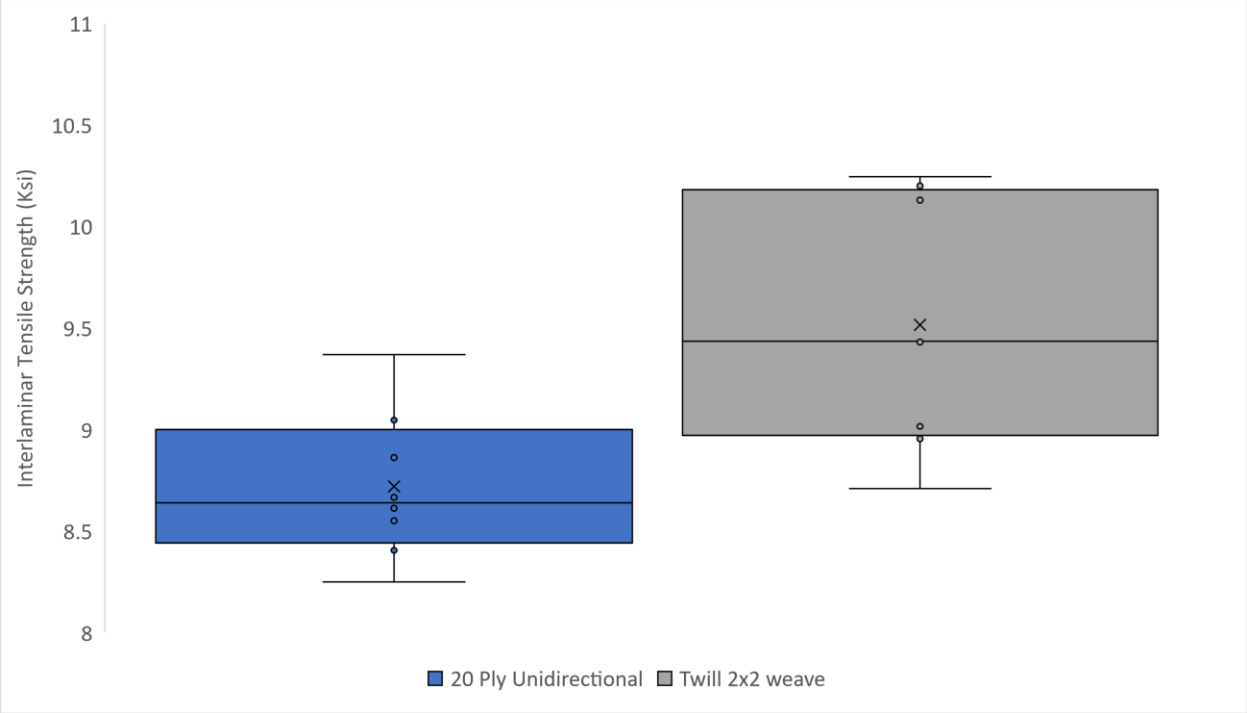

Figure 17: The interlaminar tensile strength values for the unidirectional fiber (blue) and woven fiber (grey) specimen. The unidirectional fiber specimen showed more consistent results than the woven fiber specimen. The plot range is from 8-11 Ksi.

Table I: Average Values for Unidirectional and 2x2 Twill Weave Test Specimen from ASTM D6415 Testing

Fiber Type	Maximum Load (lbs)	Crosshead Displacement (in)	Curved Beam Strength (Ksi)	Interlaminar Tensile Strength (Ksi)
Unidirectional	429.53	0.40	110.57	8.72
2x2 Twill Weave	687.37	0.32	207.20	9.52

4.4 Optical Microscopy

4.4.1 Unidirectional Fiber Optical Microscopy

Unidirectional specimens were imaged optically to determine the position of the major delamination relative to the plies and ply boundaries. Optical microscopy discovered a delamination crack at the ply boundary propagating through a 90° ply (Figure 18). This crack propagated from the upper ply boundary between 0° and 90° plies to a second ply boundary on

the lower side of the 90° ply. Image B shows another major delamination at a similar location along the bend region. The major delamination occurred typically at the second 90-degree ply boundary from the top of or from the bottom, depending on the specimen.

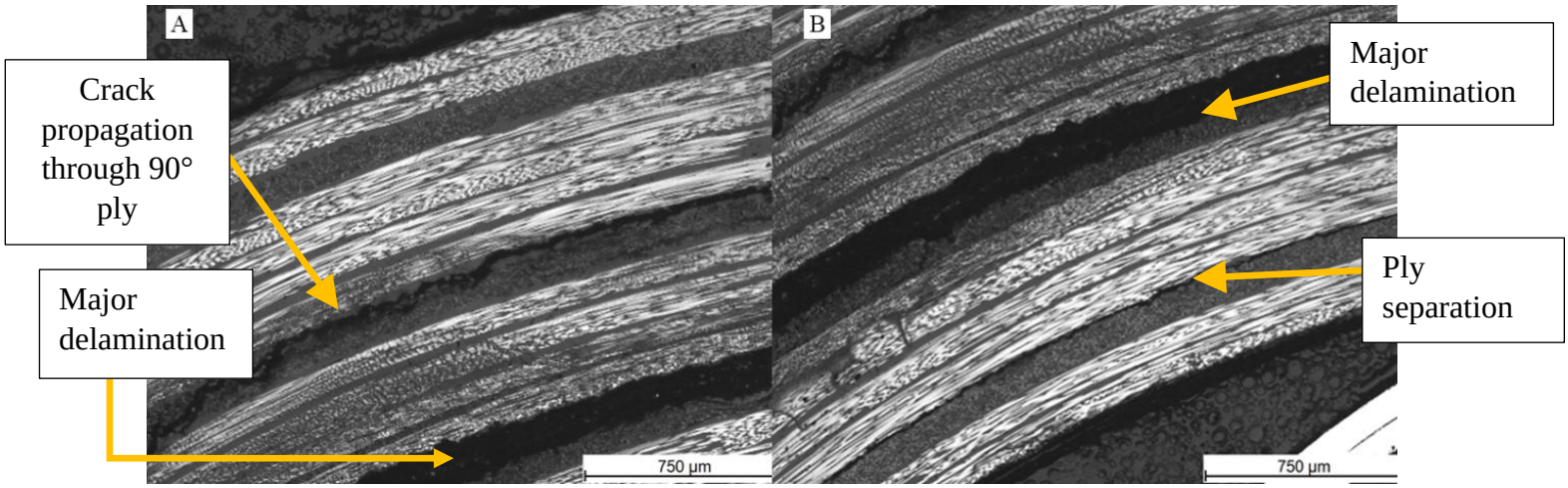

Figure 18: (a) Delamination crack propagating through 90° ply in a unidirectional laminate. (b) A delamination crack propagating along a ply boundary.

4.4.2 Woven Fiber Optical Microscopy

The delaminations found in the woven fiber specimen were located at intersections of fiber orientations within the weave (Figure 19A). In most cases, the delaminations would propagate along the fiber orientations rather than between plies. The delaminations would initiate within regions of excess matrix before propagating to along the fibers. Cracks were also found to propagate transversely through fiber tows (Figure 19B).

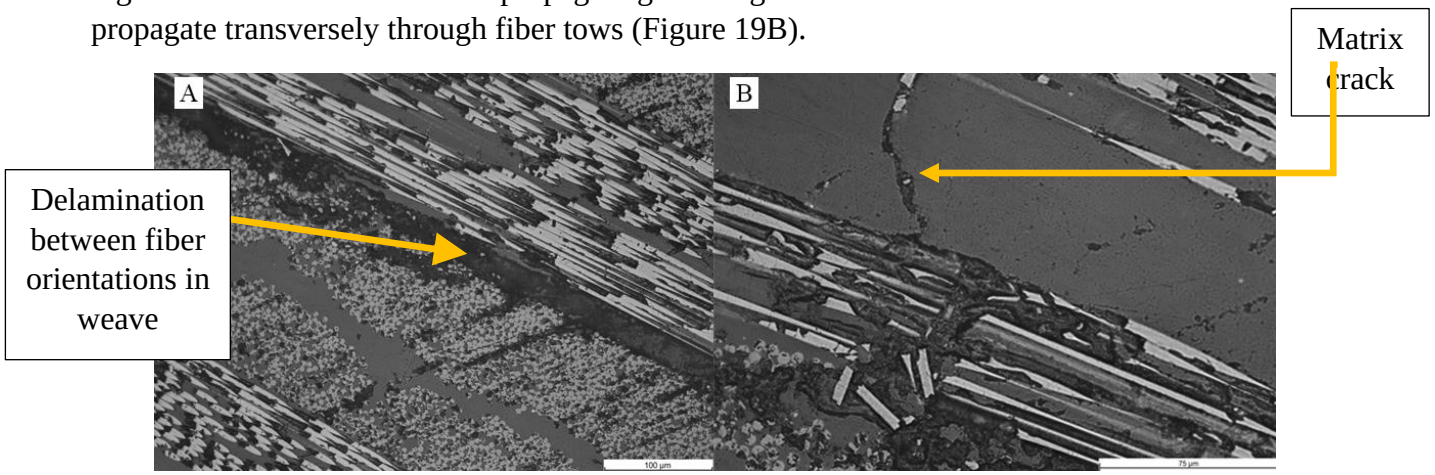

Figure 19: (A) Delamination of the woven fiber specimen at 5x showing a crack propagation along fibers in different orientations. (B) A crack initiating in a region of excess matrix before propagating through a fiber tow at 50x magnification.

4.5 Scanning Electron Microscopy

4.5.1 20-ply Unidirectional SEM

While sectioning the specimen for SEM the specimen separated along the delamination. This allowed for the fracture surfaces to be observed (Figure 20). The unidirectional fiber specimens

had a thin layer of matrix material along the center of the curved region, before propagating along the fiber surfaces (Figure 21).

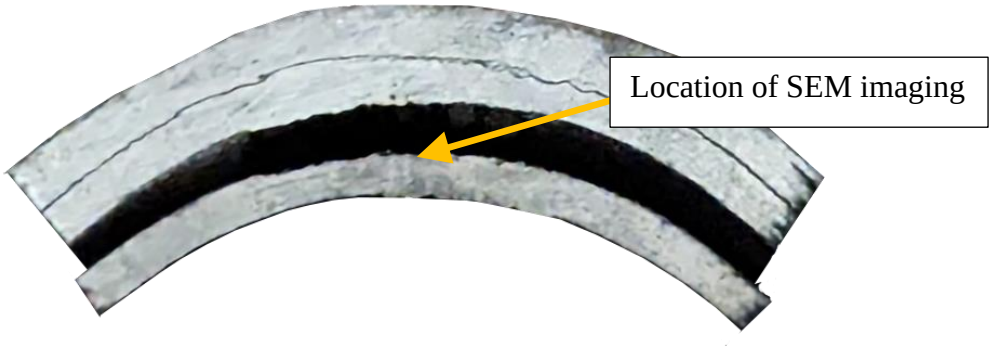

Figure 20: Side view of a sectioned SEM specimen showing where SEM images were taken.

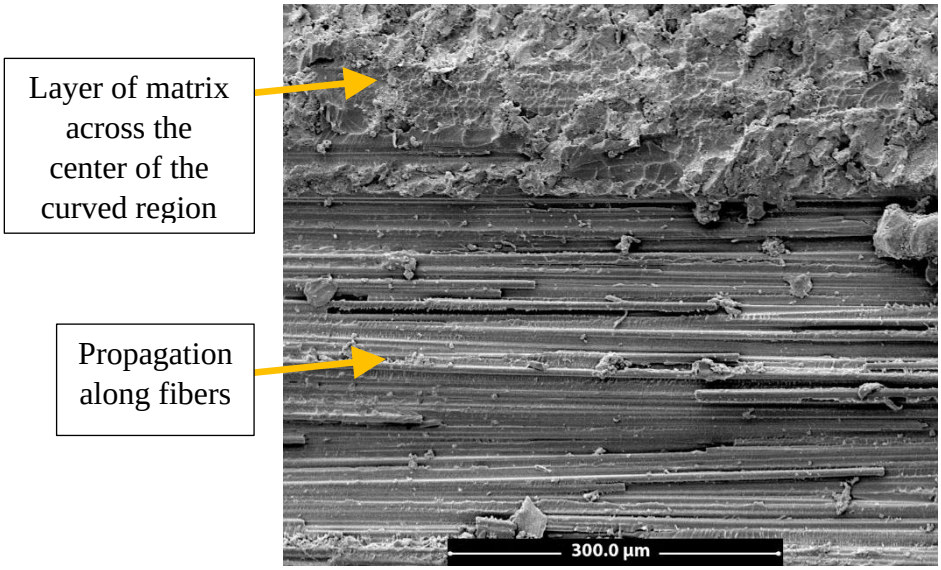

Figure 21: Low magnification SEM image of delamination fracture unidirectional specimen with layer of matrix across the center of the bent region before propagating along the fibers of a 90° ply.

At higher magnification, fibers were primarily seen with jagged pieces of matrix still attached. The jagged matrix material indicates a matrix failure had occurred. Fibers that were separated from the matrix material without matrix material were also noted, meaning that there was a mixed mode of failure within the delamination (Figure 22).

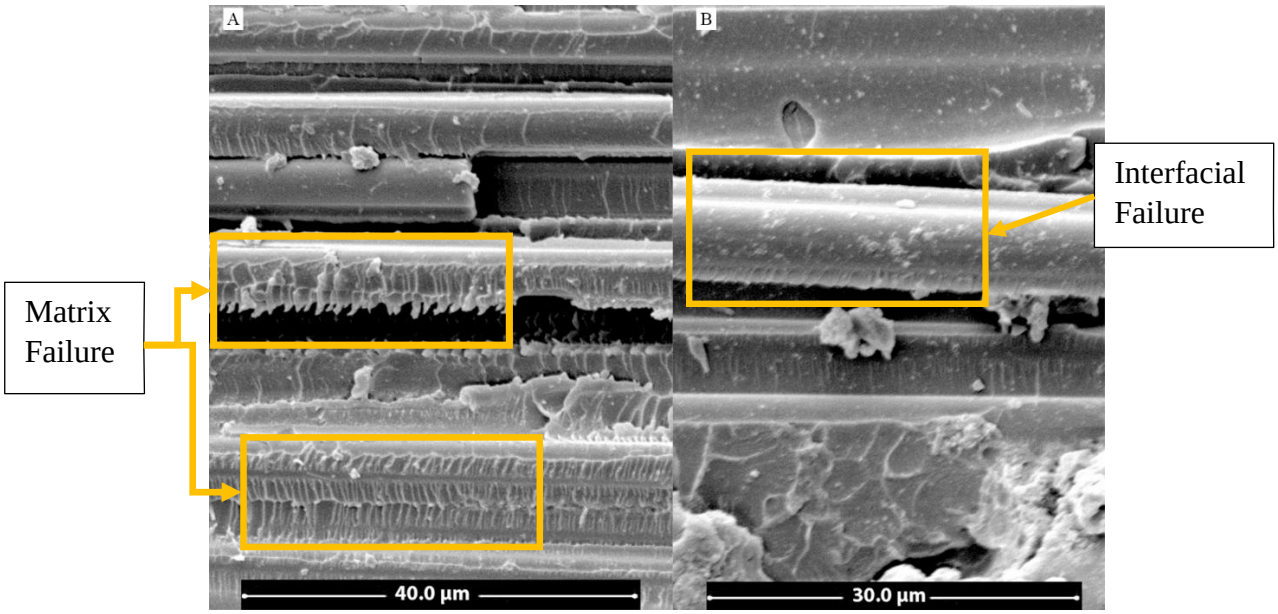

Figure 22: (A) High magnification SEM images showing matrix failure indicated by the jagged matrix material still attached to the fibers. Interfacial failure (right) was also seen where there was clean separation of the fiber from the matrix material.

4.5.2 Woven Fiber SEM

SEM analysis of the woven fiber specimens showed that the delamination most likely initiated in the regions with excess matrix within the weave, before propagating along the fibers. A large region of excess matrix between fiber orientations was seen with evidence of fibers separating from the region (Figure 23).

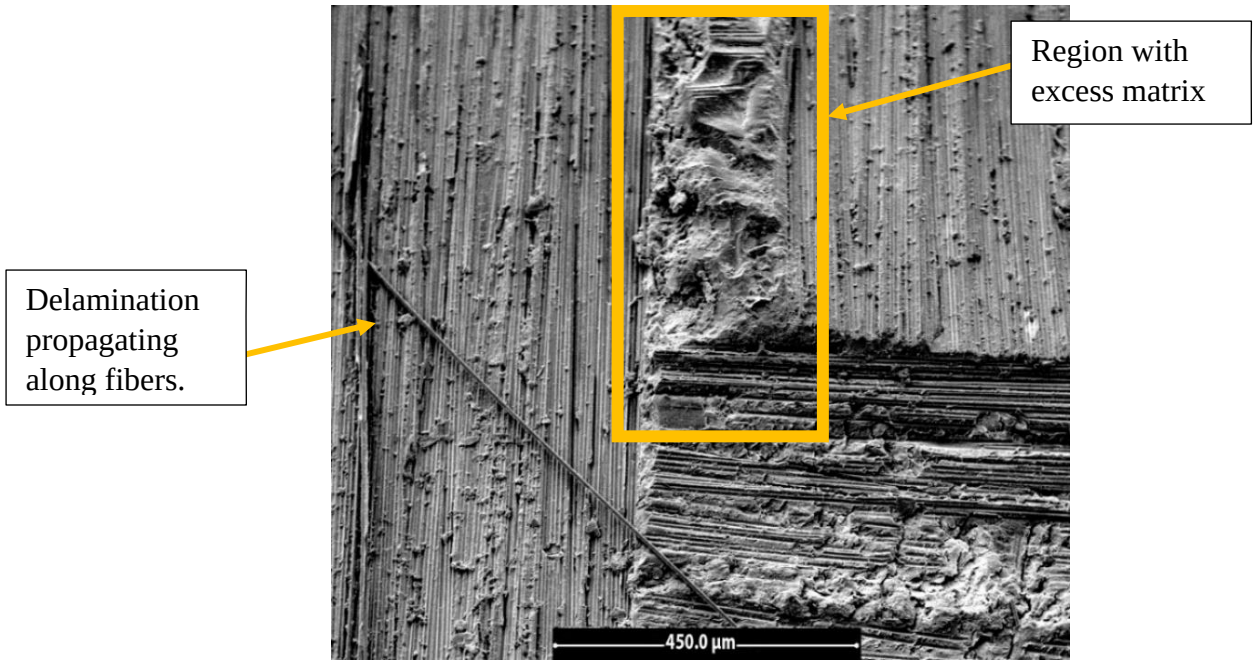

Figure 23: Low magnification image SEM image showing the region of excess matrix where fibers with different orientations meet within the 2x2 twill weave. Indentations from where fibers had separated from the matrix region can be seen. The delamination was presumed to have begun at this region of excess matrix before propagating along the layers of fiber.

The woven specimen showed more evidence of interfacial failures than the unidirectional specimen. However, there were still regions with matrix failure. Clean separation of the fibers from the matrix indicated interfacial failure and jagged matrix material indicated matrix failure (Figure 24).

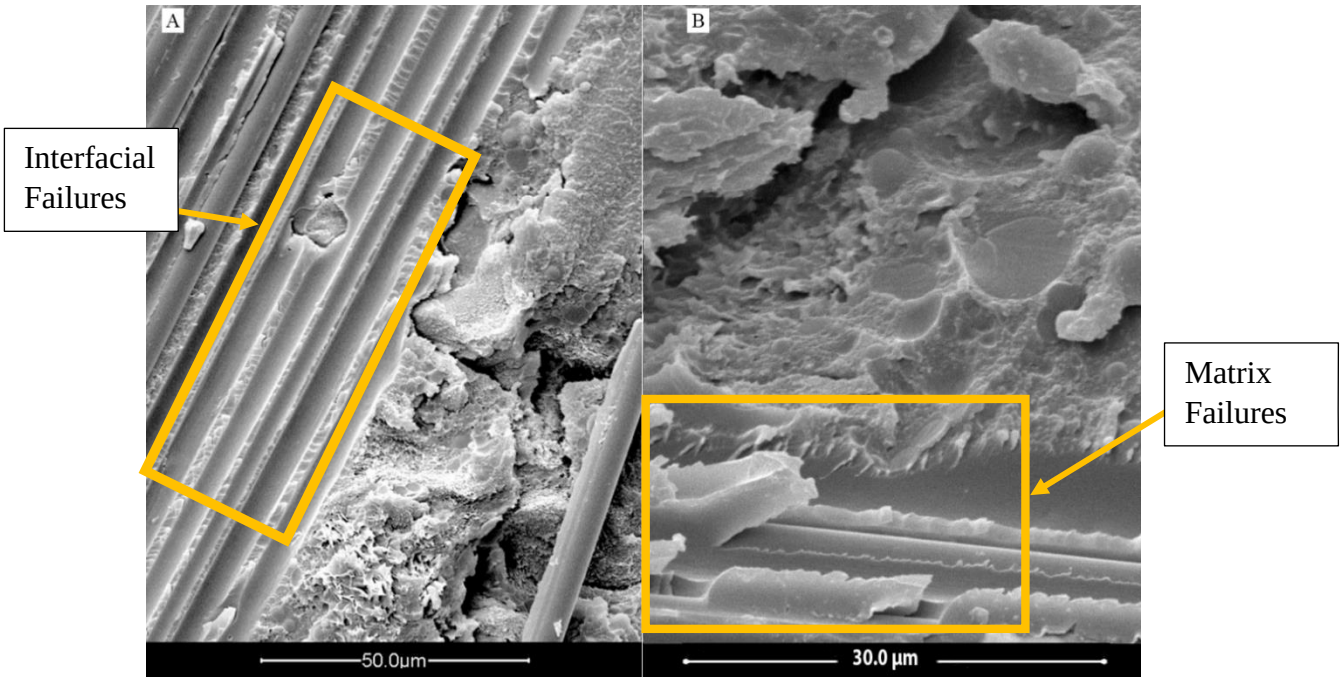

Figure 24: Higher magnification SEM images showing (A) interfacial failure and (B) matrix failures. The interfacial failures were predominantly seen with smooth surfaces where fibers had been pulled out. Matrix failures were also seen where the matrix was more jagged near the fiber separations.

5. Discussion

5.1 Interlaminar Tensile Testing

The interlaminar tensile testing was unable to produce fully accurate results during our testing. The adapter that was necessary to produce the offset resulted in a slight front to back misalignment. This misalignment resulted in uneven moments in the bend region. Therefore, the forces through the bend region would not be normal to the laminate. This could result in the delamination load presenting higher than the true value. The off-axis forces present could also produce shear stresses within the laminate that could result in an interlaminar tensile strength that is lower than anticipated.

During the woven fiber testing, there was a variation in the load applied. The load was expected to be steadily increasing with the crosshead displacement with sudden drops indicating a delamination. The cause of this variance is unclear as there are multiple potential sources for error. The first potential reason is from the front-to-back misalignment of the fixture. As the load increases, an off-axis force would be applied to the load frame. This could result in the load frame shifting and changing the alignment of forces during the test. Another potential cause for the variance is the weave of the fibers within the laminate. As the fibers are interlaced the orientation would be shifted slightly out of alignment from the curved beam. As the specimen is

flexed during testing the shifting of fibers could cause these crimps to shift into better alignment and increase the load needed for displacement and vice versa.

5.2 Optical Microscopy

The optical microscopy was able to successfully determine the location of delamination within the laminates as well as information on how they propagated. The unidirectional specimens propagated along ply boundaries in all cases with some instances of the crack propagating through the 90° plies. The woven fiber specimen showed delamination propagating along the boundaries between fiber orientations, however it was more difficult to identify the individual ply boundaries compared to the unidirectional specimens. This indicates that there was good consolidation of the plies.

5.3 Scanning Electron Microscopy

The SEM analysis of the fracture surface provided insight into the fracture mechanisms of both the unidirectional and woven fiber specimens. The unidirectional specimen showed a consistent trend of there being a thin layer of matrix across the center of the bent region before propagating along the fibers at the ply boundary. There was also further evidence of matrix failure shown by the jagged edges of matrix still attached to fibers. Lastly, there existed some evidence of interfacial failure from fibers cleanly separated from the matrix, however this was much less prevalent.

In the woven fiber specimen, there was also evidence of the fractures initiating within the matrix. The matrix heavy regions showed evidence of fractures and fiber pullout before the delamination propagated along the fibers. Unlike the unidirectional specimen, there were more instances of interfacial failure than matrix failure where fibers were separating. Most fibers separated from the matrix had smooth surfaces. There was evidence of matrix failure with the matrix appearing to tear, however this was less prevalent. It could not be determined if this difference was caused by the weave, or the different fibers used. The different fibers could have different bonding properties with the matrix because of sizing differences and thus matrix adhesion and compatibility. Additionally, the actual resin content would be different due to the difference in wettability of the fibers by the TC380 epoxy matrix, which impacts the delamination properties. This variation could result in the different fracture mechanisms seen between the samples. Sizing compositions are proprietary so they cannot be easily determined. This makes it difficult to know what the differences between them are, and if it would result in the different fracture mechanisms.

6. Conclusions

1. Delamination in unidirectional specimens displays a trend of starting in the matrix and propagating to and along the ply boundary.
2. Woven laminate appeared to fail in regions of excess matrix material at intersections of fiber orientations.
3. Woven laminate displayed more interfacial failures than unidirectional laminates.
4. ILTS for unidirectional specimens was less than the 2x2 twill weave with average ILTS values of 8.72 and 9.52 Ksi respectfully.
5. ILTS Data is unreliable due to the adapter resulting in fixture misalignment.

7. Recommendations

1. Design a fixture that does not require an offset to complete tests. Additionally, a fixture that has adjustable span lengths would allow for a wider range of specimen sizes to be tested, as well as allowing for micro adjustments to correct potential misalignments.
2. Comparing woven and unidirectional laminates with the same fiber type could provide more detail on the differences in fracture mechanism caused by the weave.

References

(1) Cook, J.; Booth, S. Carbon Fiber Manufacturing Facility Siting and Policy Considerations: International Comparison. 2017. https://www.nrel.gov/docs/fy17osti/66875.pdf.

(2) Composites, E. 6. Carbon Fiber Manufacturing Methods | Element 6 Blog. June 2022. https://element6composites.com/carbon-fiber-manufacturing-methods/#:~:text=Fiber%20Manufacturing%20Methods-.

(3) How to Manufacture Carbon Fiber Parts. https://formlabs.com/blog/composite-materials-carbon-fiber-layup/.

(4) U.S. Congress, O. of T. A. *Advanced Materials by Design.*; OTA-E-351 (Washington, DC: U.S. Government Printing Office, June 1998).

(5) Chawla, K. K. Matrix Materials; Composite Materials; 2019; pp 75–105. https://doi.org/10.1007/978-3-030-28983-6_3.

(6) Ratna, D. *Recent Advances and Applications of Thermoset Resins*, 2nd ed.; Elsevier, 2022.

(7) Mangalgiri, P. D. Composite Materials for Aerospace Applications. *Bulletin of Materials Science* **1999**, *22*, 657–664. https://doi.org/10.1007/bf02749982.

(8) Mahendran, A. R.; Wuzella, G.; Lammer, H.; Gindl-Altmutter, W. Thermosetting Natural Fiber Based Composites. *Fiber Reinforced Composites* **2021**, 187–214. https://doi.org/10.1016/b978-0-12-821090-1.00014-4.

(9) Greene, J. P. *Automotive Plastics and Composites*; Elsevier, 2021. https://doi.org/10.1016/c2018-0-03030-3.

(10) Boeing. Boeing: 787 By Design. 2016. https://www.boeing.com/commercial/787/by-design/#/advanced-composite-use.

(11) Grippi, R. Design, Fabrication, and Testing of the Applications Technology Satellite Apogee Motor Nozzle. NASA June 1967. https://ntrs.nasa.gov/api/citations/19680014539/downloads/19680014539.pdf.

(12) Chawla, K. K. Reinforcements. **1998**, 6–71. https://doi.org/10.1007/978-1-4757-2966-5_2.

(13) Watt, W. Production and Properties of High Modulus Carbon Fibres. *Proceedings of the Royal Society of London. A. Mathematical and Physical Sciences* **1970**, *319*, 5–15. https://doi.org/10.1098/rspa.1970.0161.

(14) Olliges, R. Carbon Fiber Weaves: What They Are and Why to Use Them. June 2019. https://www.elevatedmaterials.com/carbon-fiber-weaves-what-they-are-and-why-to-use-them/.

(15) Composites, A. C. P. Woven Fabric Style Guide | ACP Composites. https://store.acpcomposites.com/woven-fabric-style-guide.

(16) Drzal, L. T. The Interphase in Epoxy Composites. *Epoxy Resins and Composites II* **2005**, 1–32. https://doi.org/10.1007/bfb0017913.

(17) Fitzer, E.; Geigl, K.-H.; Hüttner, W.; Weiss, R. Chemical Interactions between the Carbon Fibre Surface and Epoxy Resins. *Carbon N Y* **1980**, *18*, 389–393. https://doi.org/10.1016/0008-6223(80)90029-9.

(18) Ma, Q.; Gu, Y.; Li, M.; Wang, S.; Zhang, Z. Effects of Surface Treating Methods of High-Strength Carbon Fibers on Interfacial Properties of Epoxy Resin Matrix Composite. *Appl Surf Sci* **2016**, *379*, 199–205. https://doi.org/10.1016/j.apsusc.2016.04.075.

(19) Li, M.; Gu, Y. Z.; Liu, H.; Li, Y. X.; Wang, S. K.; Wu, Q.; Zhang, Z. G. Investigation the Interphase Formation Process of Carbon Fiber/Epoxy Composites Using a Multiscale Simulation Method. *Compos Sci Technol* **2013**, *86*. https://doi.org/10.1016/j.compscitech.2013.07.008.

(20) Ma, J.; Jiang, L.; Dan, Y.; Huang, Y. Study on the Inter-Laminar Shear Properties of Carbon Fiber Reinforced Epoxy Composite Materials with Different Interface Structures. *Mater Des* **2022**, *214*. https://doi.org/10.1016/j.matdes.2022.110417.

(21) Yang, T.; Zhao, Y.; Liu, H.; Sun, M.; Xiong, S. Effect of Sizing Agents on Surface Properties of Carbon Fibers and Interfacial Adhesion of Carbon Fiber/Bismaleimide Composites. *ACS Omega* **2021**, *6*, 23028–23037. https://doi.org/10.1021/acsomega.1c01103.

(22) Tr J;', J.-L.; 15t, D.; Curti; Al', U. CRAG TE-ST METHODS FOR THE MEASUREMENTOF THE ENGINEERING PROPERTIES OF FIBRE REINFORCED PLASTICS Edited by " LJ]h Lf. 1988. https://apps.dtic.mil/sti/pdfs/ADA201142.pdf.

(23) Test Method for Flatwise Tensile Strength of Sandwich Constructions. *ASTM* **2017**. https://doi.org/10.1520/c0297_c0297m-16.

(24) Standard Test Method for Through-Thickness “Flatwise” Tensile Strength and Elastic Modulus of a Fiber-Reinforced Polymer Matrix Composite Material. December 2022. https://www.astm.org/d7291_d7291m-15.html.

(25) Test Method for Measuring the Curved Beam Strength of a Fiber-Reinforced Polymer-Matrix Composite. *D6415* **2022**. https://doi.org/10.1520/d6415_d6415m-22.

(26) Ciotola, F. *ASTM D6415 TESTING FIXTURE*. Sophia High Tech. https://www.sophiahightech.com/astm-d-6415-testing-fixture/ (accessed 2023-06-08).

(27) Cinar, K.; Guven, I.; Oz, F.; Ersoy, N. Quantifying the Delamination of L-Shaped Composite Laminates Under Low Velocity Impact Using X-Ray Computed Tomography. In *American Society for Composites 2018*; DEStech Publications, Inc.: Lancaster, PA, 2018. https://doi.org/10.12783/asc33/25949.

Appendix

Appendix A: 30 Ply Unidirectional Specimen

30 ply unidirectional specimens were also produced using a similar layup pattern. However, during the temperature and pressure ramp of the cure the vacuum bag burst. The laminate was left under vacuum for an entire weekend to debulk before the autoclave cure. The extended debulk was a result of the autoclave already in use. This process variation produced a laminate with seemingly good consolidation from visual and optical microscopy. Once testing began the issues with the laminate became apparent with the maximum load before delamination only being100-140 lbs (Figure 25). The average ILTS for the 30 ply specimens was 2.41 Ksi, much lower than the 20-ply unidirectional or woven specimens (Figure 26). This significant reduction in performance was most likely a result of poor consolidation not the additional plies. Delaminations occurred between most plies rather than a single major delamination. This data was omitted from the body of the report, as it would not provide an accurate representation of the materials being tested. These results are also not able to make valid comparison of unidirectional and woven fabrics. This testing does show the importance of proper curing cycles, as the poor laminate quality did not become apparent until testing. Additional tabulated test data can be studied below in Table II.

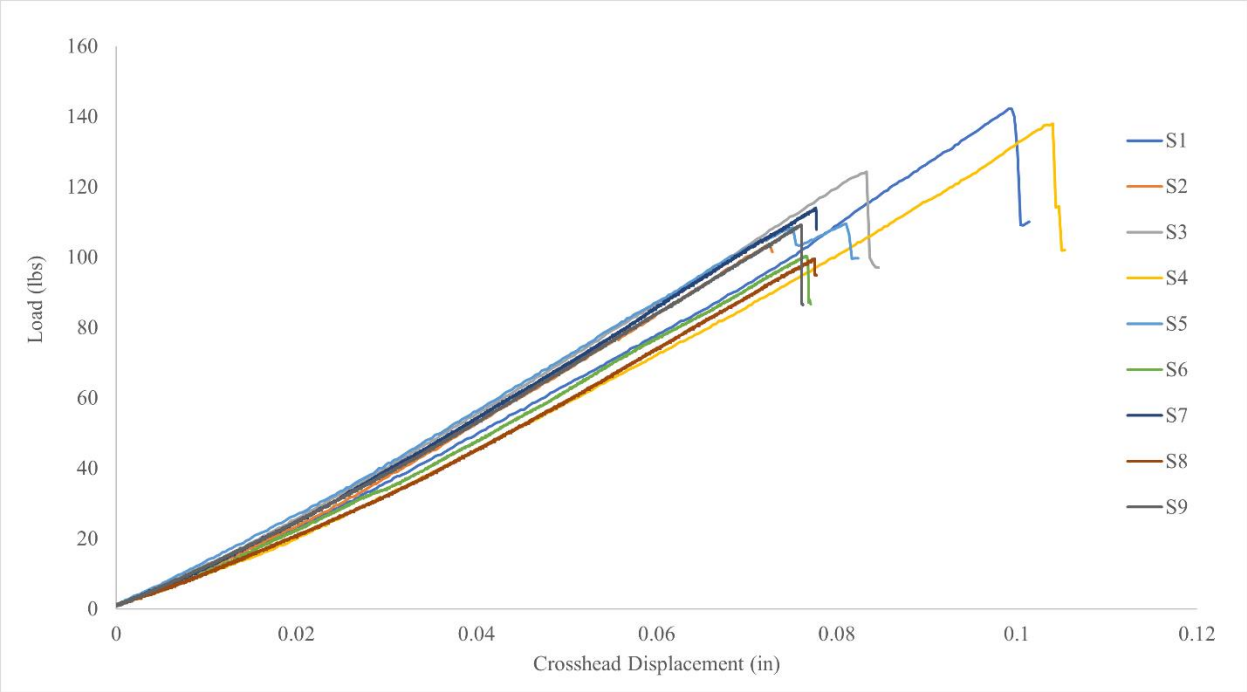

Figure 25: ASTM D6415 testing for the 30-ply unidirectional specimen. The failure loads occurred between 100 and 140 pounds at a crosshead displacement of 0.075″ and 0.11″.

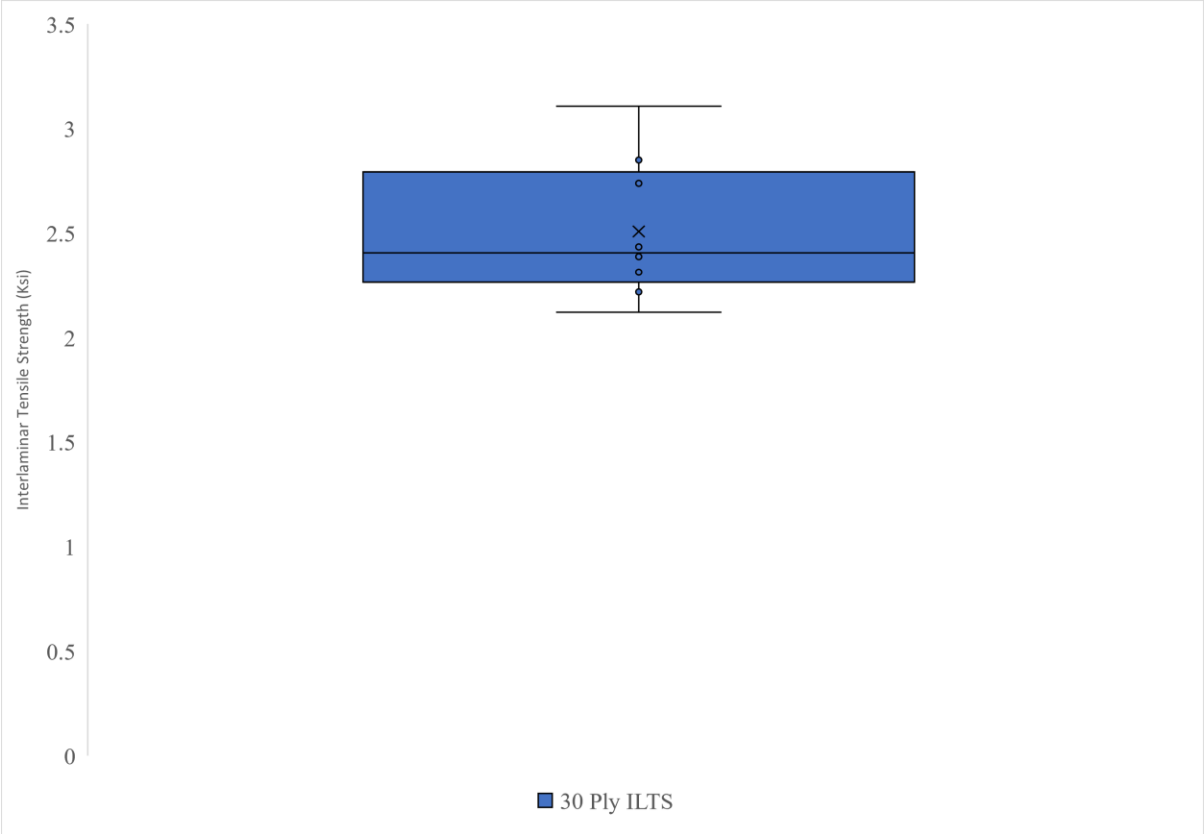

Figure 26: The 30-ply unidirectional interlaminar tensile strength ranged from 2-3 Ksi. This is much lower than the 20-ply unidirectional specimens and is most likely a result of the manufacturing issues encountered

Appendix B: Individual Specimen ASTM D6415 Test Results

Table II: 20 Ply Unidirectional ASTM D6415 Test Results

Specimen	Crosshead Displacement (in)	Maximum Load (lbs)	Curved Beam Strength (Ksi)	Interlaminar Tensile Strength (Ksi)
1	0.38	395.93	105.31	8.41
2	0.39	438.61	114.90	9.05
3	0.40	424.61	109.64	8.61
4	0.43	445.80	111.47	8.86
5	0.39	421.83	110.63	8.67
6	0.39	416.54	108.97	8.55
7	0.41	472.01	119.33	9.37
8	0.42	420.94	104.30	8.25

Table III: 2x2 Twill Weave ASTM D6415 Test Results

Specimen	Crosshead Displacement (in)	Maximum Load (lbs)	Curved Beam Strength (Ksi)	Interlaminar Tensile Strength (Ksi)
1	0.31	645.43	202.44	9.44
2	0.34	754.58	219.26	10.20
3	0.30	630.51	197.24	9.02
4	0.32	686.91	207.88	9.43
5	0.34	777.48	226.91	10.25
6	0.30	619.53	192.79	8.71
7	0.34	760.16	219.40	10.13
8	0.31	624.38	191.64	8.96

Table IV: 30 Ply Unidirectional ASTM D6415 Test Results

Specimen	Crosshead Displacement (in)	Maximum Load (lbs)	Curved Beam Strength (Ksi)	Interlaminar Tensile Strength (Ksi)
1	0.10	142.17	61.31	2.85
2	0.07	103.82	50.10	2.31
3	0.08	124.32	59.07	2.74
4	0.10	138.02	62.78	3.11
5	0.08	108.44	51.42	2.39
6	0.08	100.39	45.89	2.12
7	0.08	114.02	53.27	2.43
8	0.08	99.56	47.48	2.22
9	0.08	109.17	52.27	2.41